# Copropagation of two waves of different frequencies and arbitrary initial polarization states in an isotropic Kerr medium

E. López Lago and R. de la Fuente
*Escola Universitaria de Optica e Optometria, Departamento de Física Aplicada, Universidade de Santiago de Compostela, Galicia, Spain*
(Received 27 October 1998)

Using a circularly polarized basis, we derive the differential equations governing the copropagation of two waves of different frequencies and arbitrary initial amplitudes and polarizations in an isotropic Kerr medium, and we give exact analytical solutions for waves that are initially linearly polarized. In this latter case, the ellipticities and orientations of both polarization ellipses generally vary periodically as the waves propagate through the medium; when each wave is linearly polarized, the deviation of the orientation of its polarization ellipse from its initial value is either zero or close to its maximum value. Situations are identified in which this deviation is close to $\pi/2$, thus allowing one wave to switch the other on and off with the aid of a linear polarizer placed at the exist from the medium. All the results obtained are generalizable to copropagation in nonbirefringent optical fibers. [S1050-2947(99)02707-9]

PACS number(s): 42.65.−k, 42.81.Gs, 42.25.Ja

## I. INTRODUCTION

When several waves copropagate in a Kerr medium, there occur phase shifts that depend on the intensity of each wave. This phenomenon is called self-phase modulation (SPM) or cross-phase modulation (XPM) depending on whether the phase shift is induced by the self-interaction of each wave or by coupling among different waves. Competition between the two processes can lead to changes in the polarization of the waves. In the case of two interacting waves of the same frequency but different polarizations (degenerate XPM), the polarization ellipse of the total wave is rotated. In the case of an intense linearly polarized wave accompanied by a probe wave of different frequency, the birefringence induced by the former alters the polarization state of the latter; this effect is the nonlinear analogue of the linear birefringence effect that takes place in a retardation plate, and is generally known as light-induced linear birefringence. Since the pioneering work of Duguay and Hansen [1] on the optical Kerr gate, several all-optical devices based on light-induced linear birefringence have been proposed for purposes such as modulation, sampling, switching and amplification [2–7]. Moreover, in short light pulses nondegenerate XPM causes spectral broadening and wavelength shifts leading to timing changes and pulse shaping [8–13]. Finally, XPM can be used to allow an intense pump beam to focus or guide a probe beam [14–19], and for measurement of nonlinear indices of refraction or Kerr coefficients [20–22].

Typically, the effects and applications of nondegenerate XPM or light-induced linear birefringence have been analyzed or developed for the copropagation of an intense pump wave and a probe wave weak enough for its self-action and its effects on the pump wave to be negligible. As far as we know, the only published research on interaction between waves of similar intensities has concerned waves with mutually parallel or orthogonal linear polarization used to create a bound pair of optical solitons [23–27]; in these situations, no change in polarization occurs. In this paper, we analyze the steady-state polarization changes induced in each other and in themselves by two waves of different frequencies, arbitrary intensities and arbitrary initial polarization that copropagate in a Kerr medium. Each wave is considered to induce birefringence affecting the polarization of both. Special attention is paid to waves that are initially linearly polarized, and to the influence of the initial angle between their directions of polarization; we show that as each wave traverses the medium its state of polarization varies with a period that depends on the physical parameters characterizing the process. This effect may allow light-induced birefringence to be exploited in situations more general than the pump-and-probe configurations explored hitherto.

We note that the results of this paper are valid for both isotropic bulk media and nonpolarizing optical fibers, in which the power required for significant polarization changes is several orders of magnitude smaller due to light confinement.

The organization of the paper is as follows. In Sec. II we derive the equations governing the evolution of the amplitude and phase of each wave, and we present some conservation laws that are useful for their solution. In Sec. III we find analytical solutions for the special case of waves that are initially linearly polarized; discuss their dependence on the parameters of the medium, the relative amplitudes of the waves and the initial relative orientation of their polarization axes; and identify situations ensuring absolute changes in orientation of $\pi/2$ allowing one beam to switch the other on and off with the aid of a linear polarizer placed at the exit from the medium.

## II. THE NONLINEAR EQUATIONS

In this section we derive differential equations describing the evolution of the amplitudes and phases of two waves of frequencies $\omega_1$ and $\omega_2$ propagating along the $Z$ axis of a nonlinear isotropic Kerr medium. We write the electric field in the medium as

 

$$\vec{E}(\vec{r},t)=\vec{E}_1(z)e^{-i\omega_1 t}+\vec{E}_2(z)e^{-i\omega_2 t}+\text{c.c.} \tag{1}$$

The third-order nonlinear polarization of the medium at each frequency $\omega_j$ ($j=1,2$) may be written as the sum of two contributions, the first representing the action of the wave of the same frequency (responsible for SPM) and the second the action of the other wave (responsible for XPM):

$$\vec{P}_j^{nl}(z)=3\varepsilon_0\chi^{(3)}(\omega_j;\omega_j,\omega_j,-\omega_j)\vdots\vec{E}_j\cdot\vec{E}_j\cdot\vec{E}_j^*+6\varepsilon_0 \times\chi^{(3)}(\omega_j;\omega_j,\omega_{3-j},-\omega_{3-j})\vdots\vec{E}_j\cdot\vec{E}_{3-j}\cdot\vec{E}_{3-j}^*, \quad j=1,2. \tag{2}$$

To simplify, we neglect the frequency dependence of $\chi^{(3)}$ and write

$$\chi_{iklm}=\chi_{iklm}^{(3)}(\omega_1;\omega_1,\omega_1,-\omega_1)=\chi_{iklm}^{(3)}(\omega_2;\omega_2,\omega_2,-\omega_2),$$
$$\chi'_{iklm}=\chi_{iklm}^{(3)}(\omega_1;\omega_1,\omega_2,-\omega_2)=\chi_{iklm}^{(3)}(\omega_2;\omega_2,\omega_1,-\omega_1). \tag{3}$$

Since in an isotropic medium

$$\chi_{iklm}^{(3)}=\delta_{ik}\delta_{lm}\chi_{1122}^{(3)}+\delta_{il}\delta_{km}\chi_{1212}^{(3)}+\delta_{im}\delta_{kl}\chi_{1221}^{(3)} \tag{4}$$

(see, for example, Ref. [28]), and since intrinsic permutation symmetry may be imposed to set $\chi_{1122}=\chi_{1212}$, Eq. (2) can now be written in the form

$$\vec{P}_j^{nl}(z)=3\varepsilon_0[(\chi_{1122}+\chi_{1212})(\vec{E}_j\cdot\vec{E}_j^*)\vec{E}_j+\chi_{1221}(\vec{E}_j\cdot\vec{E}_j)\vec{E}_j^*] +6\varepsilon_0[\chi'_{1122}(\vec{E}_{3-j}\cdot\vec{E}_{3-j}^*)\vec{E}_j+\chi'_{1212}(\vec{E}_j\cdot\vec{E}_{3-j}^*)\vec{E}_{3-j} +\chi'_{1221}(\vec{E}_j\cdot\vec{E}_{3-j})\vec{E}_{3-j}^*] \tag{5}$$

or, relative to the basis composed of the circularly polarized states $\vec{e}_\pm=(\vec{x}\pm i\vec{y})/\sqrt{2}$, in the form

$$P_{j\pm}^{nl}=6\varepsilon_0\{[\chi_{1122}|E_{j\pm}|^2+(\chi_{1122}+\chi_{1221})|E_{j\mp}|^2]E_{j\pm} +[(\chi'_{1122}+\chi'_{1221})|E_{3-j\pm}|^2 +(\chi'_{1122}+\chi'_{1212})|E_{3-j\mp}|^2]E_{j\pm} +(\chi'_{1221}+\chi'_{1212})(E_{3-j\pm}E_{3-j\mp}^*)E_{j\mp}\}, \tag{6}$$

where $E_{j\pm}$ is the coefficient of $\vec{e}_\pm$ in the expression of $\vec{E}_j$ with respect to this basis:

$$\vec{E}_j(z)=E_{j+}(z)\vec{e}_+ + E_{j-}(z)\vec{e}_-. \tag{7}$$

The first term on the right-hand side of each Eqs. (6) corresponds to the SPM of the circularly polarized component, the second to degenerate (same-frequency) XPM, the following two to nondegenerate XPM coupling components with different frequencies, and the last to four-wave mixing causing energy exchange among the various field components (see below).

Equations (6) and (7) can now be introduced into the wave equation. If we ignore backward-propagating waves, considering only two forward-propagating waves with wave numbers $k_j=\omega_j n_j/c$, where $n_j$ is the linear refractive index at frequency $\omega_j$, then standard manipulations afford the coupled equations

$$\frac{\partial E_{j\pm}}{\partial z}-ik_jE_{j\pm}=i\frac{3\omega_j}{n_jc}\{[\chi_{1122}|E_{j\pm}|^2 +(\chi_{1122}+\chi_{1221})|E_{j\mp}|^2]E_{j\pm} +[(\chi'_{1122}+\chi'_{1221})|E_{3-j\pm}|^2 +(\chi'_{1122}+\chi'_{1212})|E_{3-j\mp}|^2]E_{j\pm} +(\chi'_{1221}+\chi'_{1212})(E_{3-j\pm}E_{3-j\mp}^*)E_{j\mp}\}. \tag{8}$$

These equations imply conservation of the quantities

$$C_j=|E_{j+}|^2+|E_{j-}|^2,$$
$$C_\pm=\frac{n_j}{\omega_j}|E_{j\pm}|^2+\frac{n_{3-j}}{\omega_{3-j}}|E_{3-j\pm}|^2. \tag{9}$$

Conservation of $C_j$ means that the power flow at frequency $\omega_j$ remains invariant, i.e., that the flux of photons of frequency $\omega_j$ is conserved, while the conservation of $C_+$ and $C_-$ means that the flux of photons with a given helicity (left-handedness or right-handedness) is also constant. These four conserved quantities are related by

$$\frac{n_1}{\omega_1}C_1+\frac{n_2}{\omega_2}C_2=C_++C_-\equiv I, \tag{10}$$

which states that the total photon flux is also invariant.

The conserved quantities $C_j$ and $I$ can be used to simplify the differential equations (8) by replacing $E_{j\pm}$ with the normalized field

$$U_{j\pm}=\sqrt{\frac{n_j}{\omega_jI}}E_{j\pm}\exp\left[-i\left(k_j+\frac{3\omega_j}{n_jc}(\chi_{1122}C_j +(\chi'_{1122}+\chi'_{1212})C_{3-j})\right)z\right] \tag{11}$$

and $z$ with

$$s=\frac{3\omega_1\omega_2I(\chi'_{1212}+\chi'_{1221})}{n_1n_2c}z. \tag{12}$$

Note that since $s$ scales with both $z$ and $I$, increasing the total field intensity has the same effect as increasing the length of medium traversed by the same factor. In terms of $U_{j\pm}$ and $s$, Eqs. (8) become

$$\frac{\partial U_{j\pm}}{\partial s}=i\left[\frac{\omega_jn_{3-j}}{\omega_{3-j}n_j}\mu|U_{j\mp}|^2U_{j\pm}+\nu|U_{3-j\pm}|^2U_{j\pm} +(U_{3-j\pm}U_{3-j\mp}^*)U_{j\mp}\right], \tag{13}$$

where

$$\mu=\frac{\chi_{1221}}{\chi'_{1212}+\chi'_{1221}},\quad \nu=\frac{\chi'_{1221}-\chi'_{1212}}{\chi'_{1212}+\chi'_{1221}}. \tag{14}$$

Equation (13) implies conservation of the quantity

$$\Gamma=\frac{1}{2}(U_{1+}U^*_{1-}U^*_{2+}U_{2-}+\text{c.c.})+\gamma_1|U_{1+}|^2|U_{1-}|^2 + \gamma_2|U_{2+}|^2|U_{2-}|^2, \tag{15}$$

where $\gamma_j=1/2[(\omega_j n_{3-j}/\omega_{3-j}n_j)\mu+\nu]$. Finally, writing $U_{j\pm}=a_{j\pm}e^{i\varphi_{j\pm}}$ (where $a_{j\pm}$ and $\varphi_{j\pm}$ are real) and defining $\theta=(\varphi_{2+}-\varphi_{2-})-(\varphi_{1+}-\varphi_{1-})$, we obtain the equations

$$\frac{\partial a_{j\pm}}{\partial s}=\pm(-1)^j a_{(3-j)+}a_{(3-j)-}a_{j+}\sin\theta,$$

$$a_{j\pm}\frac{\partial\varphi_{j\pm}}{\partial s}=\frac{\omega_j n_{3-j}}{\omega_{3-j}n_j}\mu a^2_{j\mp}a_{j\pm}+\nu a^2_{(3-j)\pm}a_{j\pm} + a_{(3-j)\pm}a_{(3-j)\mp}a_{j\mp}\cos\theta, \tag{16}$$

which can be reduced to the set of five coupled equations

$$\frac{\partial a_{1+}}{\partial s}=-a_{2+}a_{2-}a_{1-}\sin\theta,$$

$$\frac{\partial a_{1-}}{\partial s}=+a_{2+}a_{2-}a_{1+}\sin\theta,$$

$$\frac{\partial a_{2+}}{\partial s}=+a_{1+}a_{1-}a_{2-}\sin\theta,$$

$$\frac{\partial a_{2-}}{\partial s}=-a_{1+}a_{1-}a_{2+}\sin\theta,$$

$$\frac{\partial\theta}{\partial s}=\cos\theta\left[a_{2+}a_{2-}\left(\frac{a_{1+}}{a_{1-}}-\frac{a_{1-}}{a_{1+}}\right)+a_{1+}a_{1-}\left(\frac{a_{2-}}{a_{2+}}-\frac{a_{2+}}{a_{2-}}\right)\right] +2\gamma_1(a^2_{1+}-a^2_{1-})+2\gamma_2(a^2_{2-}-a^2_{2+}). \tag{17}$$

Note that the magnitudes of $\mu$ and $\nu$ depend on the nature of the physical process producing the optical nonlinearity. For example, if the physical mechanism is the nonresonant electronic response of bound electrons, $\mu=1/2$ and $\nu=0$. Surprisingly, the same values are taken when the nonlinearity is due to molecular orientation [29].

Note also that although Eq. (13) has been derived for bulk isotropic materials, it can be modified to apply to single-mode nonbirefringent optical fibers by introducing, on the right-hand side, an overlap integral accounting for the effective area of the mode, as can easily be shown using coupled mode theory [30]. Since $s$ can be scaled to include the modal integral, the results of this paper hold for both bulk isotropic materials and nonpolarizing optical fibers.

Equations (9), (10), and (15) are equivalent to

$$a^2_{1+}+a^2_{1-}=h_1,\quad a^2_{1+}+a^2_{2+}=h_+,$$

$$a^2_{2+}+a^2_{2-}=h_2,\quad a^2_{1-}+a^2_{2-}=h_-,$$

$$h_1+h_2=h_++h_-=1,$$

$$a_{1+}a_{1-}a_{2+}a_{2-}\cos\theta+\gamma_1 a^2_{1+}a^2_{1-}+\gamma_2 a^2_{2+}a^2_{2-}=\Gamma, \tag{18}$$

where $h_j=(n_jC_j)/(\omega_j I)$ and $h_\pm=C_\pm/I$ [the last of Eqs. (18) can be obtained from the last of Eqs. (17)].

These relations allow replacement of $\sin\theta$ and three amplitudes in the evolution equation of the remaining amplitude, and hence solution of Eqs. (17) for given initial conditions. The general solution, which can be expressed in terms of Jacobian elliptic functions, can adopt a great variety of particular forms depending on the initial polarization states and, through the parameters $\gamma_1$ and $\gamma_2$, on the frequencies and the optical characteristics of the medium. Typically, energy exchange between the waves forces changes in the polarization state with a periodicity that depends upon the initial conditions (see Fig. 1). However, there are particular sets of initial conditions for which no energy exchange takes place, and hence no polarization changes either. Inspection of Eqs. (17) shows that the $a_{j\sigma}$ ($\sigma=+,-$) remain constant when the two waves are circularly polarized, and that both the $a_{j\sigma}$ and $\theta$ remain constant when they are linearly polarized with $\theta=0$ (parallel polarization) or $\theta=\pi$ (orthogonal polarization). The invariance of two circularly polarized waves can be considered as a generalization of the well-known fact that a single circularly polarized wave does not undergo degenerate XPM in an isotropic medium [31,32]. In the next section we analyze in greater detail the behavior of waves that are linearly polarized when they enter the medium.

## III. INITIALLY LINEARLY POLARIZED WAVES

In the common case in which both waves are initially linearly polarized,

$$a^2_{1+}(0)=a^2_{1-}(0)=h_1/2,$$

$$a^2_{2+}(0)=a^2_{2-}(0)=h_2/2=(1-h_1)/2,$$

$$h_+=h_-=1/2,$$

$$\Gamma=\frac{1}{4}(h_1h_2\cos\theta_0+\gamma_1h_1^2+\gamma_2h_2^2), \tag{19}$$

where $\theta_0=\theta(0)$ is twice the angle between the directions of polarization of the two waves at the input plane of the medium. Since Eqs. (17) are invariant under the transformation ($\theta\leftrightarrow-\theta$, $a_{j+}\leftrightarrow a_{j-}$), we can restrict our analysis to $\theta_0$ values between 0 and $\pi$.

To solve Eqs. (17), we take the first of these equations and use Eqs. (18) and (19) to obtain an equation in the single variable $f=h_1/2-a^2_{1+}$ involving the constants $h_1$, $h_2$, $\cos\theta_0$ and $\gamma=\gamma_1+\gamma_2$. Then

$$-2s\sqrt{(1-\gamma^2)\rho_+}=\int_0^{y(s)}\frac{dy}{[(1-y^2)(1-my^2)]^{1/2}}, \tag{20}$$

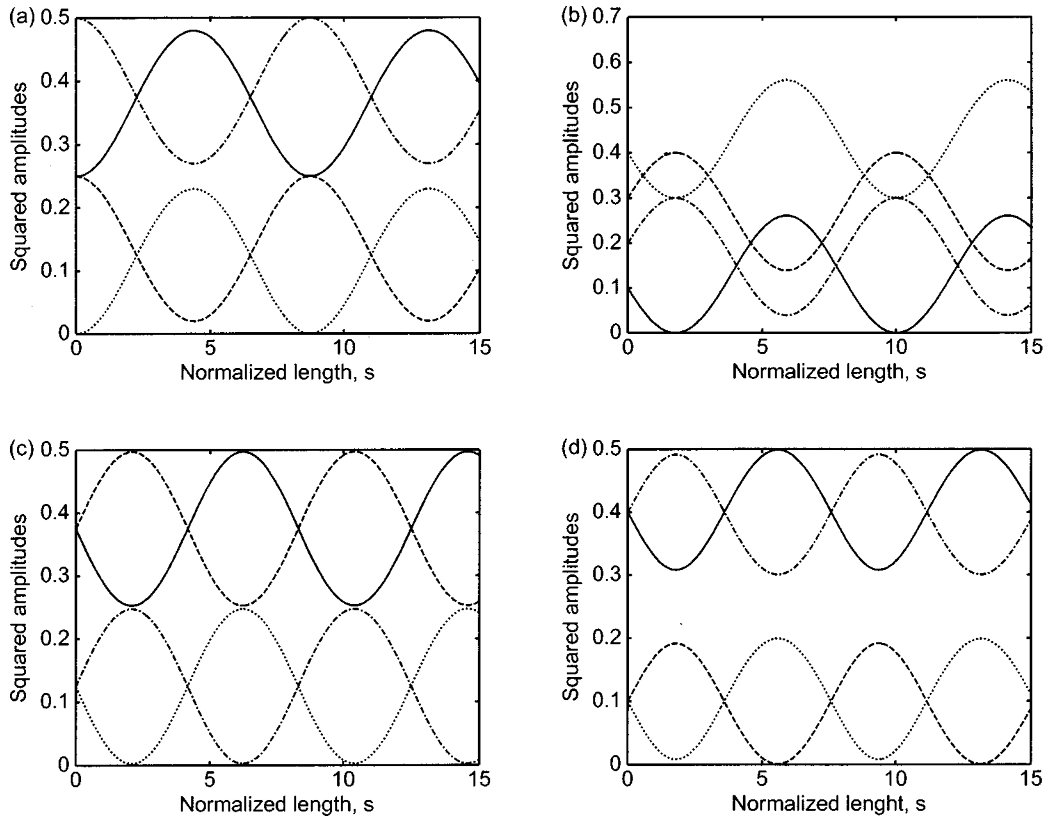


FIG. 1. Squared amplitude of each circular component as a function of the normalized lengths for the following initial conditions: (a) $a_{1+}^2(0)=a_{1-}^2(0)=0.25$, $a_{2+}^2(0)=0.5$, $a_{2-}^2(0)=0$; (b) $a_{1+}^2(0)=0.1$, $a_{1-}^2(0)=0.3$, $a_{2+}^2(0)=0.2$, $a_{2-}^2(0)=0.4$; (c) $a_{1+}^2(0)=a_{1-}^2(0)=3/8$, $a_{2+}^2(0)=a_{2-}^2(0)=1/8$; (d) $a_{1+}^2(0)=a_{2+}^2(0)=0.4$, $a_{1-}^2(0)=a_{2-}^2(0)=0.1$. In all the figures $\theta(0)=\pi/2$, $\omega_2/n_2=2\omega_1/n_1$, $\mu=0.5$, and $\nu=0$ (so $\gamma=5/8$). The solid curve corresponds to the left-handed component of wave 1, the dashed curve to its right-handed component, the dashed-dotted curve to the left-handed component of wave 2, and the dotted curve to the right-handed component of wave 2.

where $y(s)=-f/\sqrt{\rho_-}$ and $m=\rho_-/\rho_+$, $\rho_+$ and $\rho_-$ being the roots of $(h_1^2/4-f^2)(h_2^2/4-f^2)-[(h_1h_2\cos\theta_0)/4+\gamma f^2]^2=0$ considered as a quadratic in $f^2$:

$$\rho_\pm=\frac{1}{4(1-\gamma^2)}\left\{\frac{1}{2}+h_1h_2(\gamma\cos\theta_0-1)\right.$$
$$\left.\pm\left[\frac{1}{4}+h_1h_2(\gamma\cos\theta_0-1)+h_1^2h_2^2(\cos\theta_0-\gamma)^2\right]^{1/2}\right\}. \tag{21}$$

Since the integral on the right-hand side of Eq. (20) is the elliptic integral of the first kind with amplitude $\sin^{-1}(y)$ and modulus $\sqrt{m}$, the amplitudes $a_{j\pm}(s)$ are given in terms of the Jacobian elliptic function sn by

$$a_{1\pm}^2(s)=h_1/2\mp\sqrt{\rho_-}\,\mathrm{sn}(2s\sqrt{(1-\gamma^2)\rho_+}|\rho_-/\rho_+),$$
$$a_{2\pm}^2(s)=h_2/2\pm\sqrt{\rho_-}\,\mathrm{sn}(2s\sqrt{(1-\gamma^2)\rho_+}|\rho_-/\rho_+) \tag{22}$$

so long as $0\leq m<1$. By the definition of $\rho_\pm$, this condition is satisfied if $\gamma^2<1$, since then $0\leq\rho_-<\rho_+$. If $\gamma^2>1$, in which case $\rho_+\leq 0\leq\rho_-$ and $m<0$, then it is convenient to express the $a_{j\pm}(s)$ in terms of the Jacobi elliptic function sd=sn/dn of squared modulus $m'=-m/(1-m)=\rho_-/(\rho_--\rho_+)>0$ [33]:

$$a_{1\pm}^2(s)=h_1/2\mp\sqrt{\frac{\rho_-\rho_+}{\rho_+-\rho_-}}\,\mathrm{sd}(2s\sqrt{(\gamma^2-1)(\rho_--\rho_+)}|m'),$$
$$a_{2\pm}^2(s)=h_2/2\pm\sqrt{\frac{\rho_-\rho_+}{\rho_+-\rho_-}}\,\mathrm{sd}(2s\sqrt{(\gamma^2-1)(\rho_--\rho_+)}|m'). \tag{23}$$

When $\gamma^2=1$ we can obtain the solution by taking the limits of the following parameters involved in Eq. (22):

$$\lim_{\gamma^2\to 1}\frac{\rho_-}{\rho_+}=0,$$
$$\lim_{\gamma^2\to 1}2\sqrt{(1-\gamma^2)\rho_+}=[1+2h_1h_2(\cos\theta_0\gamma-1)]^{1/2},$$
$$\lim_{\gamma^2\to 1}\sqrt{\rho_-}=\frac{h_1h_2\sin\theta_0}{2[1+2h_1h_2(\cos\theta_0\gamma-1)]^{1/2}} \tag{24}$$

and since $\mathrm{sn}(x|0)=\sin(x)$, Eqs. (22) become

$$a_{1\pm}^2(s)=\frac{h_1}{2}\left(1\mp\frac{h_2\sin\theta_0}{\rho}\sin(\rho s)\right),$$
$$a_{2\pm}^2(s)=\frac{h_2}{2}\left(1\pm\frac{h_1\sin\theta_0}{\rho}\sin(\rho s)\right), \tag{25}$$

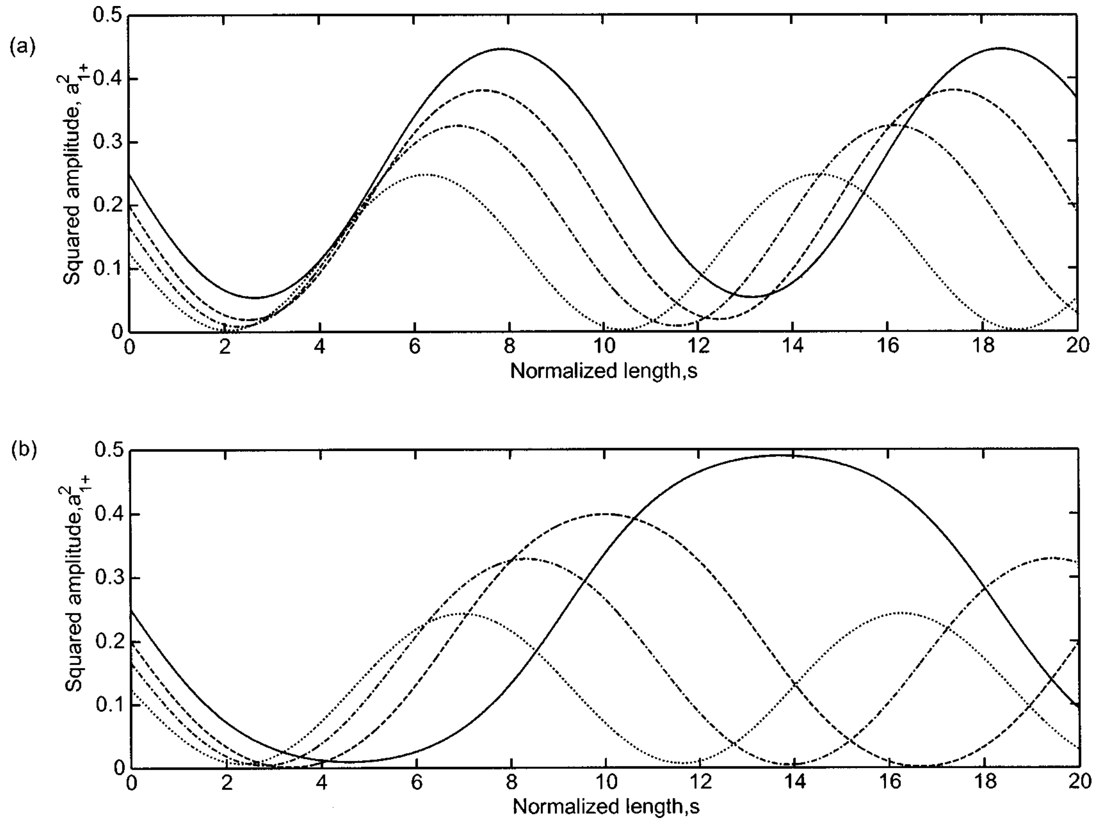


FIG. 2. Squared amplitude $a^2_{1+}$ as a function of the normalized length. (a) $\theta_0 = \pi/2$; (b) $\theta_0 = 2\pi/3$. We have taken $\gamma = 5/8$ and the values of $h_1$ are as follows: $h_1 = 1/2$ (solid curve), $h_1 = 2/5$ (dashed curve), $h_1 = 1/3$ (dashed-dotted curve), and $h_1 = 1/4$ (dotted curve).

where $\rho = [1 + 2h_1h_2(\cos\theta_0\gamma - 1)]^{1/2}$. Finally $\theta(s)$ is retrieved from Eqs. (18) and (19) as

$$\theta(s) = \cos^{-1}\left(\frac{h_1h_2\cos\theta_0/4 + \gamma f^2(s)}{\sqrt{[h_1^2/4 - f^2(s)][h_2^2/4 - f^2(s)]}}\right). \quad (26)$$

In Figs. 2 and 3 we plot $a^2_{1\pm}(s)$ and $\theta(s)$ for several values of the physical parameters involved. All the variables depend periodically on $s$, with a period $T(\cos\theta_0, h_1)$ given by the properties of the Jacobian elliptic functions as

$$T = \frac{2}{\sqrt{(1-\gamma^2)\rho_+}}\int_0^1 \frac{dy}{(1-y^2)(1-my^2)}$$

$$= \frac{2K(m)}{\sqrt{(1-\gamma^2)\rho_+}}, \quad \gamma^2 < 1,$$

$$T = \frac{2\pi}{\rho}, \quad \gamma^2 = 1,$$

$$T = \frac{2K(m)}{\sqrt{(\gamma^2 - 1)(\rho_- - \rho_+)}}, \quad \gamma^2 > 1, \quad (27)$$

where $K(m)$ stands for the complete elliptic integral of the first kind. The $a^2_{j\pm}$ vary between the extremes $(h_j/2 \pm \sqrt{\rho_-})$. The range of variation of $\theta$ depends on the relation between $\cos\theta_0$ and $-\gamma\min(h_1,h_2)/\max(h_1,h_2)$. Assuming, without loss of generality, that $h_1 \leqslant h_2$, then if $\cos\theta_0 > -\gamma h_1/h_2$, $\theta$ varies from $\theta_0$ at $s=0$ to 0 at $s=T/4$ and goes on decreasing to $-\theta_0$ at $s=T/2$. If, on the other hand, $\cos\theta_0 < -\gamma h_1/h_2$, then $\theta$ increases from $\theta_0$ at $s=0$ to $\pi$ at $s=T/4$ and finally reaches the value $2\pi - \theta_0$ at $s=T/2$.

If $\cos\theta_0 = -\gamma h_1/h_2$, closer analysis is required. In this case $\rho_- = h_1^2/4$ (the maximum value it can attain under variation of $\cos\theta_0$ for fixed $\gamma$ and $h_1$), $\rho_+ = (h_2\sin\theta_0)^2/4(1-\gamma^2)$, and if $\gamma^2 < 1$ the solutions obtained for the amplitudes [Eqs. (22)] reduce to

$$a^2_{1\pm}(s) = \frac{h_1}{2}[1 \mp \mathrm{sn}((1-h_1)\sin(\theta_0)s|m)],$$

$$a^2_{2\pm}(s) = \frac{h_2}{2} \pm \frac{h_1}{2}\mathrm{sn}((1-h_1)\sin(\theta_0)s|m), \quad (28)$$

where $m = [(1-\gamma^2)/\gamma^2]\cot^2(\theta_0)$. Substitution into Eq. (26) now gives

$$\cos\theta(s) = -\gamma\frac{|\mathrm{cn}(s(1-h_1)\sin\theta_0|m)|}{\sqrt{h_2^2/4 - \mathrm{sn}^2(s(1-h_1)\sin\theta_0|m)}}, \quad (29)$$

which means that when $s=T/4$, $\theta$ jumps from $\pi/2$ to $-\pi/2$. This jump coincides with the point at which $a_{1+}$ becomes zero [see Eq. (28)] and $\partial a_{1+}/\partial s$ changes sign from negative to positive [see Eq. (17)]. From this point on, $\theta$ decreases further to attain the value $-\theta_0$ at $s=T/2$. However, if $h_1 = h_2$, $\theta$ remains constant at its initial value, $\cos^{-1}(-\gamma)$.

As noted above, Eq. (28) implies that if $s=(2n+1)T/4$ ($n$ an integer), one of the two circularly polarized components of the wave of frequency $\omega_1$ vanishes. However, if $h_1$

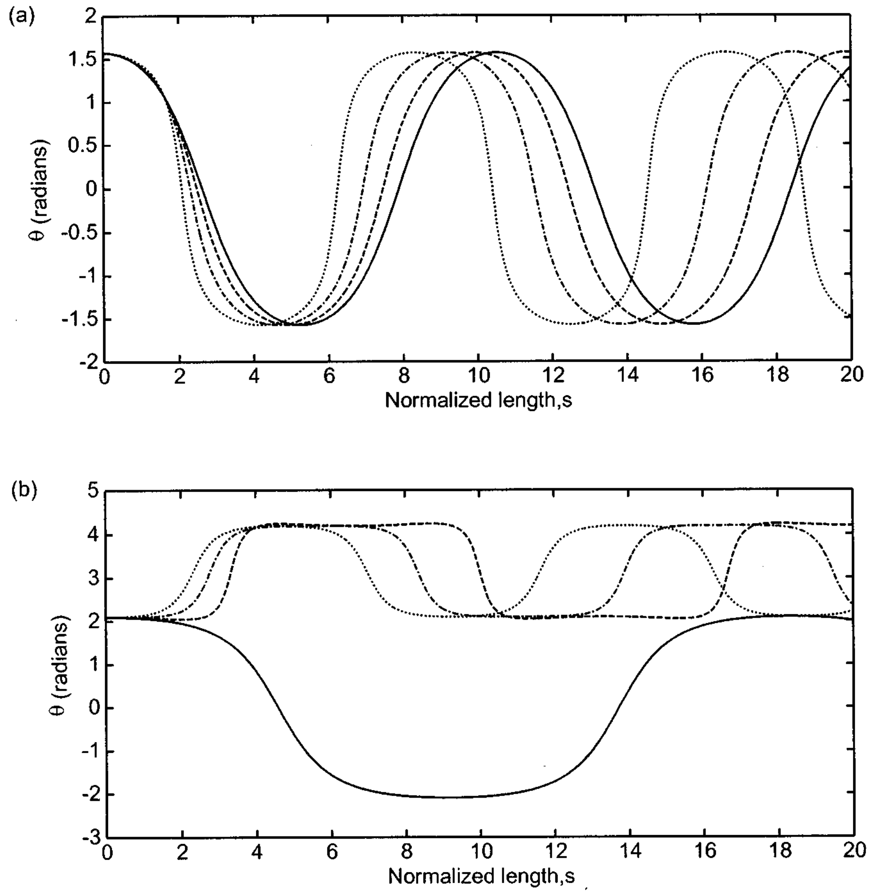


FIG. 3. Evolution of $\theta$ as a function of the normalized length. The parameters are the same as in Fig. 2.

approaches the value 1/2, then $\cos\theta_0$ decreases to $-\gamma$ (we are still assuming that $\cos\theta_0=-\gamma h_1/h_2$), $m$ goes to 1, $K(m)$ increases without bound, and so too does the period of the waves [see Eq. (27)], with the result that wave 1 only becomes circularly polarized at infinity. In fact, at $m=1$ Eq. (28) becomes

$$a_{j\pm}^2(s)=\frac{1}{2}[1\mp\tanh(\sqrt{1-\gamma^2}s/2)] \tag{30}$$

and since the hyperbolic tangent tends to 1 as its argument approaches infinity, both waves evolve asymptotically from linear polarization towards circular polarization. Since we have chosen $0\leq\theta_0\leq\pi$, wave 1 evolves towards right-handed circular polarization and wave 2 becomes increasingly left-handed; the reverse would happen if we took $\pi\leq\theta_0\leq 2\pi$.

Similar analyses can be carried out for the cases $\gamma^2>1$ and $\gamma^2=1$.

The polarization state of each normalized wave is characterized by the ellipticity and orientation of its polarization ellipse. The evolution of the ellipticity $e_j=|(a_{j+}^2-a_{j-}^2)/(a_{j+}^2+a_{j-}^2)|$ follows immediately from the results obtained above: $e_j(s)=f^2(s)/h_j$. The orientation of the major axis of the polarization ellipse of wave $j$ with respect to the $X$ axis, i.e., the azimuth $\psi_j$, is given by $\psi_j=(\varphi_{j+}-\varphi_{j-})/2\equiv\Delta\varphi_j/2$. By Eqs. (16) and (19),

$$\frac{\partial\Delta\varphi_j}{\partial s}=2(\gamma_1-\gamma_2)f(s)+(-1)^{j-1}\frac{1}{2}(h_1h_2\cos\theta_0+\gamma h_j^2)\times\frac{f(s)}{h_j^2/4-f^2(s)} \tag{31}$$

and these equations can be integrated using the properties and mutual relationships of the Jacobian elliptic functions [33,34]: for $\gamma^2<1$,

$$\Delta\varphi_j(s)=\Delta\varphi_j(0)+\frac{1}{\sqrt{1-\gamma^2}}\left\{(\gamma_1-\gamma_2)\ln\left[\frac{\mathrm{dn}(x|m)-m^{1/2}\,\mathrm{cn}(x|m)}{1-m^{1/2}}\right]+(-1)^{j-1}\frac{h_1h_2\cos\theta_0+\gamma h_j^2}{\sqrt{(h_j^2-4\rho_-)(4\rho_+-h_j^2)}}[\tan^{-1}(\sqrt{m\zeta})-\tan^{-1}(\sqrt{m\zeta}\,\mathrm{cd}(x|m))]\right\}, \tag{32}$$

where $x=2s\sqrt{(1-\gamma^2)\rho_+}$ and $\zeta=(4\rho_+-h_j^2)/(h_j^2-4\rho_-)$; for $\gamma^2=1$

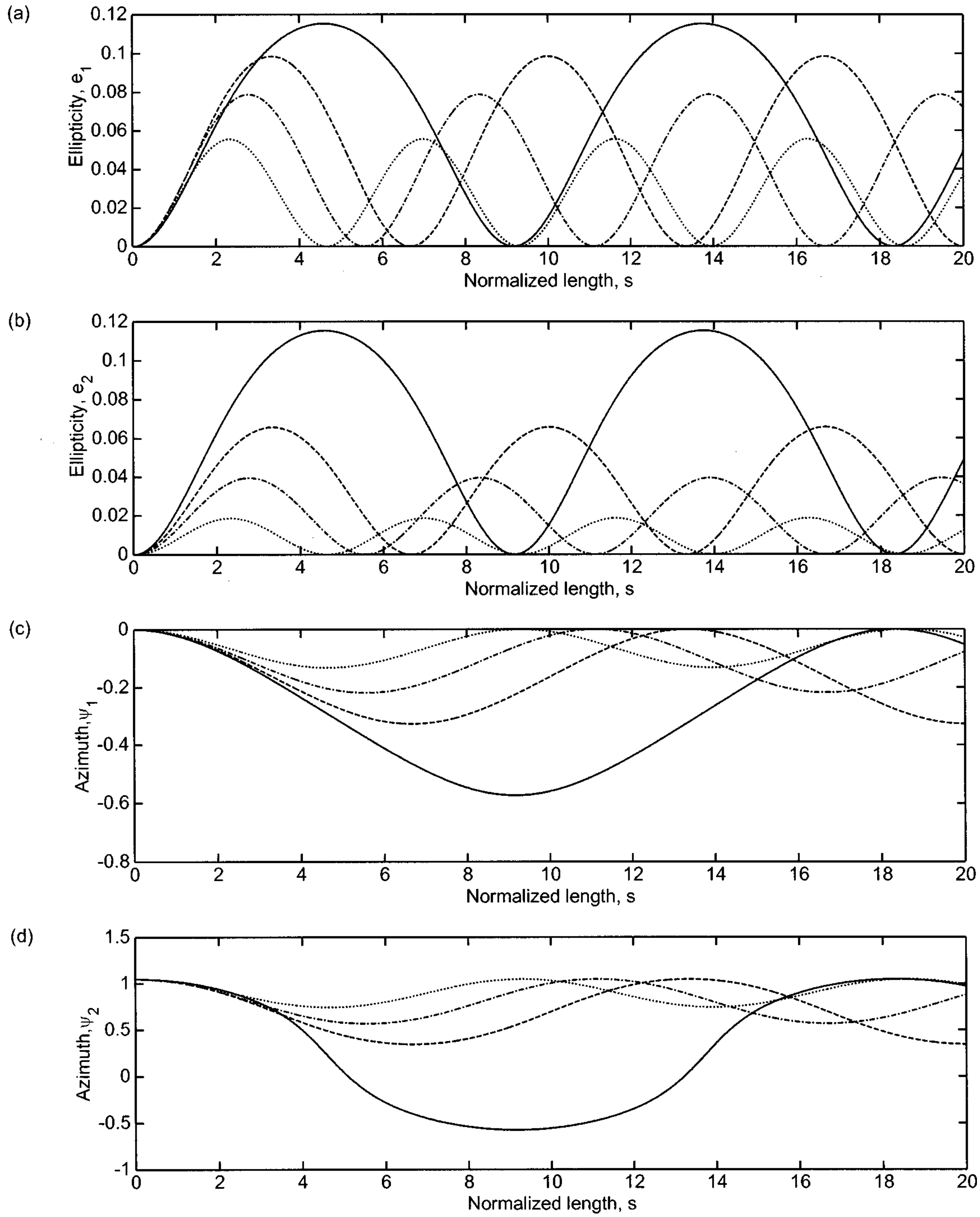


FIG. 4. Ellipticity and azimuth of each wave as a function of the normalized length for the same $h_1$ values as in Figs. 2(b) and 3(b). $[\varphi_1(0)=0;\ \varphi_2(0)=\theta_0=2\pi/3.]$

$$\Delta\varphi_j(s)=\Delta\varphi_j(0)+\left\{(\gamma_1-\gamma_2)\frac{h_1h_2\sin\theta_0}{\rho^2}(1-\cos\rho s)+(-1)^{j-1}\frac{h_1h_2\cos\theta_0+\gamma h_j^2}{\sqrt{(\rho h_j)^2-(h_1h_2\sin\theta_0)^2}}[\tan^{-1}(\xi)-\tan^{-1}(\xi\cos\rho s)]\right\}, \tag{33}$$

where $\xi=\sqrt{h_1h_2\sin\theta_0/[(\rho h_j)^2-(h_1h_2\sin\theta_0)^2]}$; for $\gamma^2>1$

$$\Delta\varphi_j(s)=\Delta\varphi_j(0)+\frac{1}{\sqrt{\gamma^2-1}}\left\{(\gamma_1-\gamma_2)[\sin^{-1}(m'^{1/2})-\sin^{-1}(m'^{1/2}\,\mathrm{cd}(x|m'))]\right.$$
$$\left.+(-1)^{j-1}\frac{h_1h_2\cos\theta_0+\gamma h_j^2}{\sqrt{(h_j^2-4\rho_-)(h_j^2-4\rho_+)}}[\tan^{-1}(\sqrt{m}\zeta)-\tan^{-1}(\sqrt{m}\zeta\,\mathrm{cn}(x|m'))]\right\}, \tag{34}$$

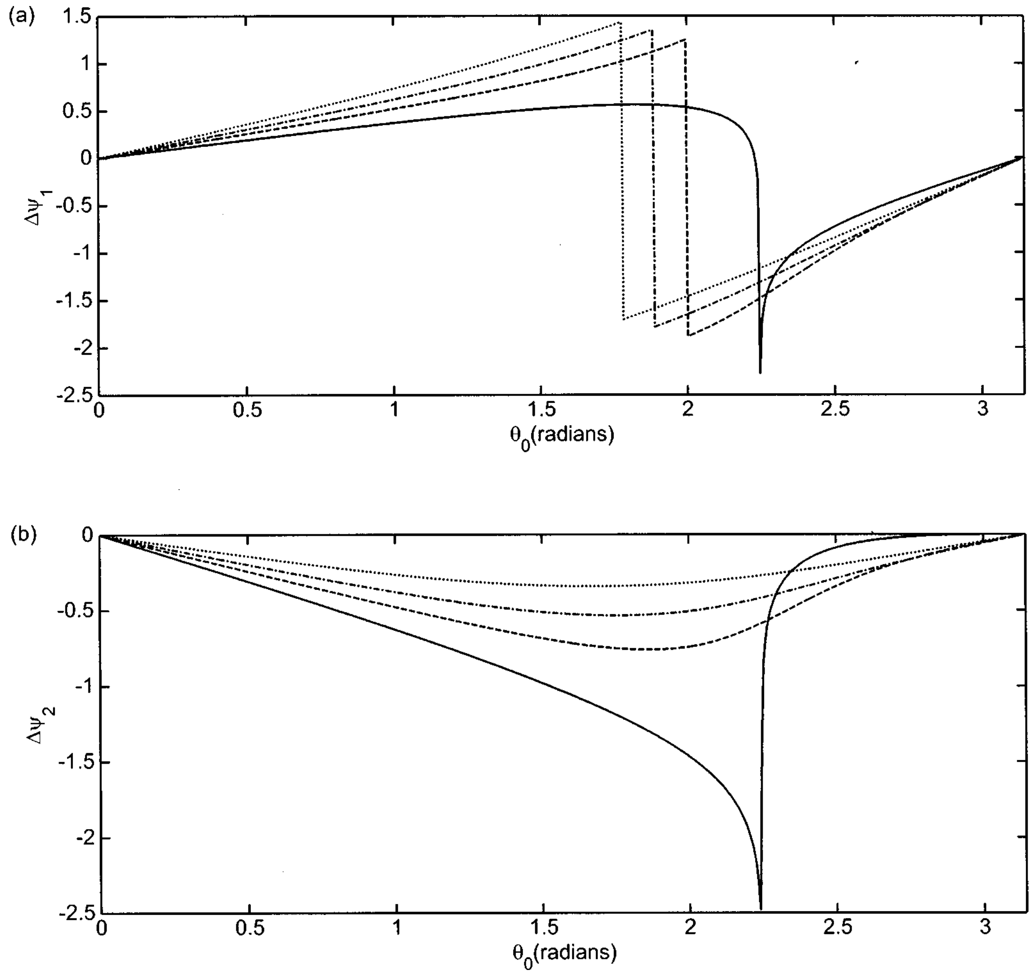


FIG. 5. Azimuth variation at $s=T/2$ as a function of the input phase difference $\theta_0$, for $h_1$ as in Fig. 2, $\omega_2/n_2=2\omega_1/n_1$, $\mu=0.5$, and $\nu=0(\gamma=5/8)$.

where $x=2s\sqrt{(\gamma^2-1)(\rho_- - \rho_+)}$ and $\zeta$ and is defined as above.

Figure 4 shows the evolution of ellipticities and azimuths under the same conditions as in Figs. 2(b) and 3(b). The orientations vary with period $T$ and the ellipticities with period $T/2$. When $s$ is an odd multiple of $T/2$, each wave is linearly polarized and the deviation of its azimuth from its initial value, $\Delta\psi_j=\psi_j(T/2)-\psi_j(0)$, is maximum or close to its maximum. Because of the periodicity of the elliptic functions, Eqs. (32) and (34) imply that in the generic situations $\gamma^2<1$ and $\gamma^2>1$,

$$\Delta\psi_j=\frac{\gamma_1-\gamma_2}{\sqrt{1-\gamma^2}}h(m)+(-1)^{j-1}\times\frac{h_1h_2\cos\theta_0+\gamma h_j^2}{\sqrt{(1-\gamma^2)(h_j^2-4\rho_-)(4\rho_+-h_j^2)}}\times\tan^{-1}(\sqrt{m\zeta}), \tag{35}$$

where

$$h(m)=\begin{cases}\tanh^{-1}(\sqrt{m}) & \text{if } \gamma^2<1\\ \sin^{-1}(\sqrt{-m'}) & \text{if } \gamma^2>1\end{cases}. \tag{36}$$

In typical applications of light-induced linear birefringence a polarizer is placed at the exit from the nonlinear medium, so that the amount of light passing the polarizer depends on the light-induced polarization undergone in the medium. For full optical switching, the polarization ellipse must be rotated by $\pi/2$. Figures 5 and 6 suggest that this value will be attained by $|\Delta\psi_j|$ if $\theta_0\approx\cos^{-1}(-\gamma h_1/h_2)$ (we assume as before that $h_1\leqslant h_2$); this is the $\theta_0$ region in which the curves for $h_1<h_2$ in Figs. 5 and 6 show a sharp drop in $\Delta\psi_1$. In fact, writing $\cos\theta_0=-\gamma(1+\delta)h_1/h_2$, Taylor expansion of Eq. (35) affords

$$\Delta\psi_j\approx\frac{\gamma_1-\gamma_2}{\sqrt{1-\gamma^2}}h(m)+\mathrm{sgn}(\delta)\frac{\pi}{2}. \tag{37}$$

Thus $\Delta\psi_j$ can always be made to achieve the value $\pi/2$ by suitable choice of the sign of $\delta$, regardless of the first term on the right of Eq. (35). If $\cos\theta_0=-\gamma h_1/h_2$ and $h_1<h_2$, we know already that at $s=T/4$ $\theta$ jumps from $+\pi/2$ to $-\pi/2$ because the left-handed component of wave 1 undergoes a phase shift of $\pi$ when it vanishes. This change in $\varphi_{1+}$ means that $\psi_j$ changes by $\pi/2$, and this change is carried forward from $s=T/4$ to $s=T/2$, so that

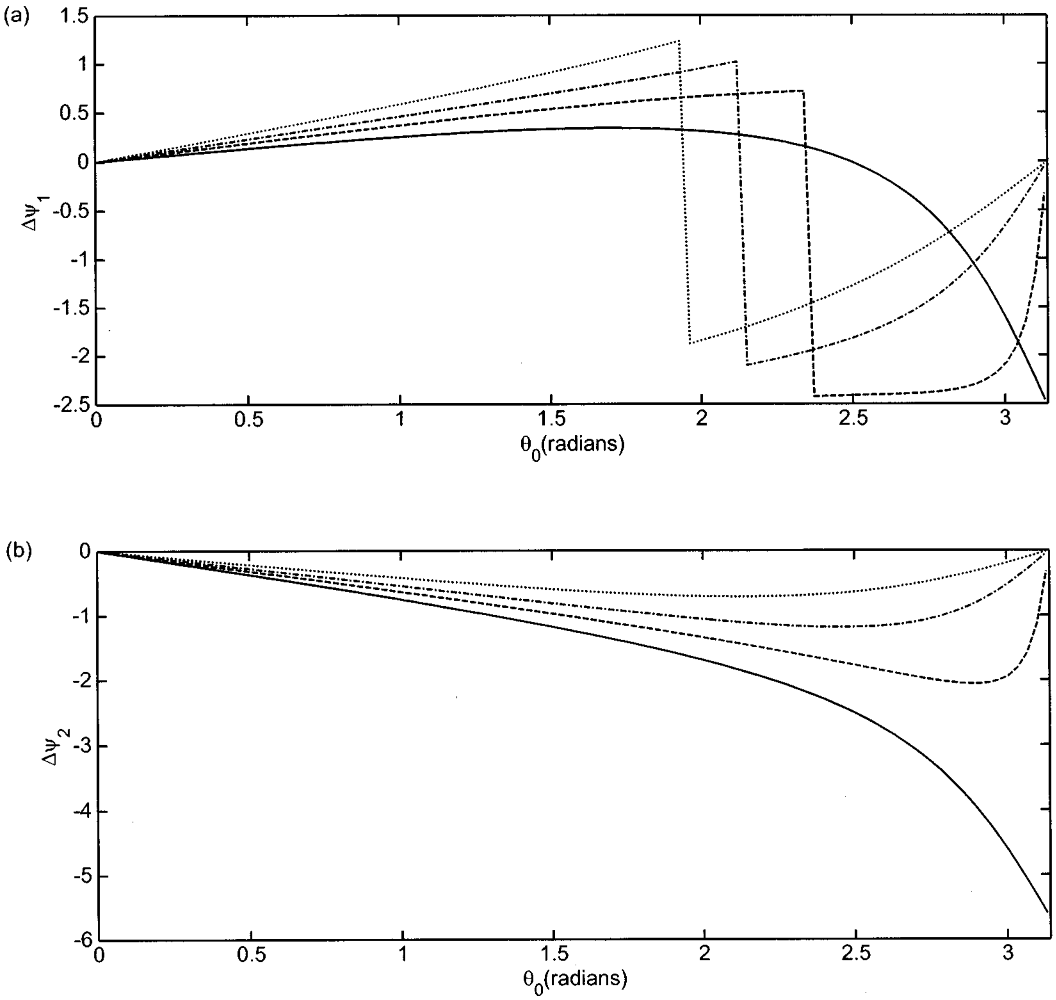


FIG. 6. As for Fig. 5, except that $\omega_2/n_2 = 4\omega_1/n_1$ and $\gamma = 17/16$.

$$\Delta\psi_1 = \frac{\gamma_1 - \gamma_2}{\sqrt{1-\gamma^2}} h(m) + \frac{\pi}{2}. \tag{38}$$

Thus if $\cos\theta_0 = -\gamma h_1/h_2$ and $h_1 < h_2$, the rotation of the polarization ellipse of wave 1 will be roughly $\pi/2$ if the first term on the right of Eq. (38) is made small by $\gamma_2$ approaching $\gamma_1$, i.e., by $w_2/n_2$ approaching $w_1/n_1$.

Equations (35) and (36) also show that if $(\gamma_1-\gamma_2)/(1-\gamma^2)^{1/2}$ is not too small, another situation in which $|\Delta\psi_j|$ can attain values close to $\pi/2$, or at least values large enough for switching purposes, is when $m$ approaches unity ($\gamma^2 < 1$) or $m'$ approaches unity ($\gamma^2 > 1$). If $\gamma^2 < 1$, $m$ can only approach unity if $h_1 \approx h_2$ [because $\rho_+/\rho_- = m \approx 1$ implies $1/4 + h_1h_2(\gamma\cos\theta_0 - 1) + h_1^2h_2^2(\cos\theta_0 - \gamma)^2 \approx 0$, and the result of solving this quadratic in $\cos\theta_0$ must be real]; this case is therefore of little interest, because in this case $\cos\theta_0 \approx -\gamma$ and so $T$ tends to infinity as $h_2$ approaches $h_1$ (since $\cos\theta_0 \approx -\gamma$, this is in fact the limiting case corresponding to the discussion of the previous paragraph, in consonance with which Fig. 5 shows that for both waves the $\theta_0$ dependence of $\Delta\psi_j$ is qualitatively of the same kind as previously discussed for wave 1). If $\gamma^2 > 1$, $m'$ approaches unity as $\rho_+$ approaches zero, which occurs if $\theta_0 \approx \pi$ and $h_1h_2(1+\gamma) \geqslant 0.5$. If $\rho_+$ is exactly zero (which corresponds to waves with mutually orthogonal polarization: $\theta = \theta_0 = \pi$), then $f(s) = 0$ [by Eq. (23)], $\Delta\varphi_j$ is constant [Eq. (31)], and $\Delta\psi_j$ is zero (as we have already seen in Sec. II). In the neighborhood of $\rho_+ = 0$, however, $|\Delta\psi_j|$ can be very large for both waves, as Fig. 6 illustrates. We conclude that the configuration in which the two waves have mutually orthogonal polarization is highly unstable under perturbation of the angle between the polarization axes. Since the first term on the right of Eq. (35) depends on $\gamma_1 - \gamma_2$, the above analysis predicts that $|\Delta\psi_j|$ may be large even though $m'$ is relatively small. This will happen if the two waves have very different frequencies. In this case, however, the assumption that the nonlinear susceptibility is independent of frequency may not be valid.

## IV. CONCLUSIONS

Equations (17) are the differential equations governing the copropagation of two waves of different frequencies and arbitrary initial amplitudes and polarizations in an isotropic Kerr medium. The exact analytical solutions given in Sec. III for the case in which the waves are initially linearly polarized show that their amplitudes and the ellipticities and orientations of their polarization ellipses vary periodically as the waves propagate through the medium in such a way that when each wave is linearly polarized, the deviation of the orientation of its polarization ellipse from its initial value is either zero or close to its maximum value. The period $T$ of the propagation pattern depends on the initial values of the intensities of the waves and of the relative orientation of their polarization axes, as does the value of $\Delta\psi_j$, the deviation in the directions of polarization which occurs at distances $(2n+1)T/2$ from the start of the medium ($n$ an integer). Situations can occur in which $\Delta\psi_j$ is close to $\pi/2$, thus allowing one wave to switch the other on and off with the aid of a linear polarizer placed at the exit from a medium of length $(2n+1)T/2$. All the above results are readily generalizable to copropagation in nonbirefringent optical fibers.

## ACKNOWLEDGMENT

This research was supported by the Xunta de Galicia under Grant No. XUGA 22901A98.


[1] M. A. Duguay and J. W. Hansen, Appl. Phys. Lett. **15**, 192 (1969).

[2] J. M. Dzedzic, R. H. Stolen, and A. Ashkin, Appl. Opt. **20**, 1403 (1981).

[3] K. Kitayama, Y. Kimura, K. Okamoto, and S. Seikai, Appl. Phys. Lett. **46**, 623 (1985).

[4] N. J. Halas, D. Krökel, and D. Grischkowsky, Appl. Phys. Lett. **50**, 886 (1987).

[5] J. H. White and R. W. Penty, Electron. Lett. **24**, 6 (1988).

[6] A. S. Davison and I. H. White, Opt. Lett. **14**, 802 (1989).

[7] C. H. Kwak, W. Y. Hwang, J. S. Jeong, H. H. Suh, and E. H. Lee, Appl. Opt. **33**, 3189 (1994).

[8] R. R. Alfano, Q. X. Li, T. Jimbo, J. T. Manassah, and P. P. Ho, Opt. Lett. **11**, 626 (1986).

[9] R. R. Alfano, P. L. Baldeck, F. Raccah, and P. P. Ho, Appl. Opt. **26**, 3491 (1987).

[10] M. N. Islam, L. F. Mollenauer, R. H. Stolen, J. R. Simpson, and H. T. Shang, Opt. Lett. **12**, 625 (1987).

[11] P. L. Baldeck and R. R. Alfano, Appl. Phys. Lett. **52**, 1939 (1988).

[12] S. G. Dinev and A. A. Drieschuh, IEEE J. Quantum Electron. **28**, 1384 (1992).

[13] G. R. Boyer, M. A. Franco, M. Lachgar, B. Grèzes-Besset, and A. Alexandrou, J. Opt. Soc. Am. B **11**, 1451 (1994).

[14] J. T. Manassah, Opt. Lett. **14**, 396 (1989).

[15] R. R. Alfano, P. L. Baldeck, P. P. Ho, and G. P. Agrawal, J. Opt. Soc. Am. B **6**, 824 (1989).

[16] G. P. Agrawal, J. Opt. Soc. Am. B **7**, 1072 (1990).

[17] S. G. Dinev, A. A. Dreischuh, and A. M. Naidenov, J. Opt. Soc. Am. B **8**, 2128 (1991).

[18] R. de la Fuente and A. Barthelemy, IEEE J. Quantum Electron. **28**, 547 (1992).

[19] A. J. Stentz, M. Kauranen, J. J. Maki, G. P. Agrawal, and R. W. Boyd, Opt. Lett. **17**, 19 (1992).

[20] R. L. Sutherland, *Handbook of Nonlinear Optics* (Dekker, New York, 1996).

[21] L. Amato, A. Fellegara, P. Sacchetto, P Boffi, A. Melloni, and M. Martinelli, Opt. Lett. **21**, 612 (1996).

[22] G. Rodríguez and A. J. Taylor, Opt. Lett. **23**, 858 (1998).

[23] S. Trillo, S. Wabnitz, E. M. Wright, and G. I. Stegeman, Opt. Lett. **13**, 871 (1988).

[24] V. V. Afanasjev, E. M. Dianov, and V. N. Serkin, IEEE J. Quantum Electron. **25**, 2656 (1989).

[25] P. C. Subramaniam, Opt. Lett. **16**, 1560 (1991).

[26] R. de la Fuente and A. Barthelemy, Opt. Commun. **88**, 419 (1992).

[27] Y. S. Kivshar, Opt. Lett. **17**, 1322 (1992).

[28] R. W. Boyd, *Nonlinear Optics* (Academic Press, New York, 1992), p. 165.

[29] Assuming dispersionless nonlinear susceptibilities. See, for example, Ref. [28].

[30] See, for example, H. Kolgenik, in *Guided-wave Optoelectronics*, edited by T. Tamir (Springer-Verlag, Berlin, 1988).

[31] P. D. Maker, R. W. Terhune, and C. M. Savage, Phys. Rev. Lett. **12**, 507 (1964).

[32] A. Owyoung, R. W. Hellwarth, and N. George, Phys. Rev. B **5**, 628 (1972).

[33] J. Spanier and K. B. Oldham, *Atlas of Functions* (Hemisphere Publishing Corporation, Washington, DC, 1987).

[34] D. F. Lawden, *Elliptic Functions and Applications* (Springer-Verlag, Berlin, 1989).